EPA-600/3-76-073
July 1976

Ecological Research Series

A DIFFRACTION TECHNIQUE TO MEASURE SIZE DISTRIBUTION OF LARGE AIRBORNE PARTICLES

Environmental Sciences Research Laboratory
Office of Research and Development
U.S. Environmental Protection Agency
Research Triangle Park, North Carolina 27711

RESEARCH REPORTING SERIES

Research reports of the Office of Research and Development, U.S. Environmental Protection Agency, have been grouped into five series. These five broad categories were established to facilitate further development and application of environmental technology. Elimination of traditional grouping was consciously planned to foster technology transfer and a maximum interface in related fields. The five series are:

1. Environmental Health Effects Research
2. Environmental Protection Technology
3. Ecological Research
4. Environmental Monitoring
5. Socioeconomic Environmental Studies

This report has been assigned to the ECOLOGICAL RESEARCH series. This series describes research on the effects of pollution on humans, plant and animal species, and materials. Problems are assessed for their long- and short-term influences. Investigations include formation, transport, and pathway studies to determine the fate of pollutants and their effects. This work provides the technical basis for setting standards to minimize undesirable changes in living organisms in the aquatic, terrestrial, and atmospheric environments.

This document is available to the public through the National Technical Information Service, Springfield, Virginia 22161.

EPA-600/3-76-073
June 1976

A DIFFRACTION TECHNIQUE TO MEASURE SIZE DISTRIBUTION OF LARGE AIRBORNE PARTICLES

by

A. McSweeney
Georgia Institute of Technology
Engineering Experiment Station
Atlanta, Georgia 30332

Grant No. R-802214

Project Officer

T. G. Ellestad
Aerosol Research Branch
Environmental Sciences Research Laboratory
Research Triangle Park, North Carolina 27711

ENVIRONMENTAL SCIENCES RESEARCH LABORATORY
OFFICE OF RESEARCH AND DEVELOPMENT
U.S. ENVIRONMENTAL PROTECTION AGENCY
RESEARCH TRIANGLE PARK, NORTH CAROLINA 27711

DISCLAIMER

This report has been reviewed by the Environmental Sciences Research Laboratory, U.S. Environmental Protection Agency, and approved for publication. Approval does not signify that the contents necessarily reflect the views and policies of the U.S. Environmental Protection Agency, nor does mention of trade names or commercial products constitute endorsement or recommendation for use.

ABSTRACT

The purpose of the work described in this report was to test and demonstrate a coherent optical diffraction technique for measuring the size distribution of large particles. This technique is based on the generation of a transformation matrix which is used to relate the measured diffraction patterns to the size distribution of the samples that produced the patterns.

Four different types of samples were considered: 1) pinholes in opaque discs, 2) photographic transparencies with opaque circular spots, 3) particles deposited on microscope slides, and 4) aerosols. Computer simulations were performed to assess the accuracy of determining particle size distributions by the optical diffraction pattern technique under both ideal and nearly ideal conditions. The results of the computer simulations indicated that it should be possible to resolve the size range from 5 to 100 μm diameter into eight subintervals.

Although good results were obtained with an array of circular apertures in an opaque background, experimental difficulties limited the precision of this technique applied to particles in a transparent medium. Expected improvements based on a reduction of system noise and an increase in detector sensitivity are discussed, and applied to the requirements on number density and size range of particles in a transparent medium.

The results obtained on this program will facilitate the design of an effective system for measuring the size distribution of particles by either of two techniques: 1) diffraction pattern analysis, or 2) Hodkinson's (ratio of measurement at two angles) technique.

CONTENTS

ABSTRACT iii

FIGURES vi

TABLES vii

ABBREVIATIONS AND SYMBOLS ix

I. INTRODUCTION 1

II. SUMMARY 10

III. CONCLUSIONS 11

IV. RECOMMENDATIONS 12

V. EXPERIMENTAL PLAN 13

VI. METHODS, PROCEDURES, RESULTS, AND DISCUSSIONS 15

REFERENCES 41

BIBLIOGRAPHY 42

FIGURES

Number		Page
1.	Basic Optical System for Producing and Measuring Diffraction Patterns	3
2.	Complete Diffraction Pattern Particle Sizing System	16

TABLES

Number		Page
1.	Circular-Aperture Diffraction Pattern Parameters	5
2.	Particle Sizes for Which the First Minimum in the Diffraction Patterns Occurred at Successive Detector Rings	22
3.	Ordered Eigenvalues of Covariance Matrix Obtained from the First Criterion	23
4.	Particle Sizes for Which Successive Diffraction Pattern Minima and Maxima Occurred at Detector Ring 32	24
5.	Ordered Eigenvalues of Covariance Matrix Obtained from the Second Criterion	25
6.	Metal Pinhole Diameters and the Ordered Eigenvalues of the Covariance Matrix	25
7.	Uniformly Spaced Aperture Diameters and the Associated Ordered Eigenvalues	26
8.	Particle Diameters for Uniformly Spaced Diffraction Maxima and the Associated Ordered Eigenvalues	27
9.	Results of Normalization of the Uniformly Spaced Diffraction Patterns	28
10.	Results of the Sixth Criterion	29
11.	Results of Normalization on the Sixth Criterion	30
12.	Specified and Measured Metal Pinhole Diameters	31
13.	Metal Pinhole Diameters Measured by Location of Diffraction Minima	33
14.	Experimental Results from Metal Pinholes	34
15.	Results from Normalized Experimental Data	34
16.	Results of Elimination of Diffraction Pattern Data for One Pinhole	35

TABLES (Continued)

Number		Page
17.	Comparison of Experimental and Computer Simulation Results	36
18.	Experimental Results from Photographic Samples	38
19.	Application of Experimentally Derived Inversion Matrix to Measured Diffraction Pattern Data	39

ABBREVIATIONS AND SYMBOLS

a - radius of particle or aperture

AR - anti-reflection

cm - centimeter, 10^{-2} meter

d - diameter of particle or aperture

EFL - effective focal length

f - focal length

G() - kernel function in integral equation

G^T - transpose of matrix G

I - irradiance (power/area)

$J_1()$ - first order Bessel function of the first kind

k - wavenumber, $\frac{2\pi}{\lambda}$

λ - wavelength

m - parameter associated with diffraction patterns See Table 1.

mm - millimeter, 10^{-3} meter

μm - micrometer, 10^{-6} meter

n - number density (particles per unit volume)

N - number of particles or apertures

nm - nanometer, 10^{-9} meter

PIN - positive - intrinsic - negative

r - radial distance from optic axis

RSI - Recognition Systems, Inc.

UDT - United Detector Technology

W - Watt

SECTION I

INTRODUCTION

The purpose of the work reported here has been to quantitatively evaluate a technique for measuring the size distribution of large particles in air. The technique is relatively new and not widely used. Major advantages are that the particle number densities can be relatively large and that the size distribution can be obtained in real-time. In general the evaluation has been directed toward obtaining quantitative values for such parameters as the optimum particle size and particle number-resolution of the technique, and then to compare these with the requirements of one specific problem: the measurement of the number vs. size of large particles in air. There may be other problems for which this technique is better suited but the purpose of this work has been to evaluate the performance in terms of the problem stated above.

The most important element in the technique is the use of coherent laser radiation to form the diffraction pattern of a group of particles exposed to the laser beam. The complicated diffraction pattern is made up of the superposition of all the diffraction patterns due to the individual particles. This conglomerate diffraction pattern is then measured and analyzed to yield the size distribution of the particles in the sample. This is referred to as an indirect measurement. The corresponding direct measurement would consist of measuring the size of each particle individually and then inferring the size distribution from the accumulated results. This could be accomplished with an optical microscope and adequate time. The indirect measurement consists of inferring the size distribution from the measured superposition of all the diffraction patterns. This can be done essentially in real-time but with some loss in precision.

This indirect method is analogous to Fourier transform spectroscopy, in which the power spectrum is measured indirectly. The resultant of the controlled superposition of all the components of the spectra is first measured and then inverted to yield the power spectrum. The advantage of Fourier spectroscopy over conventional spectroscopy is that during the measurement interval information is collected on every component in the spectrum. In conventional spectroscopy each element of the spectrum is scanned in sequence so that the effective integration time, and hence signal-to-noise ratio, is lower for the same total measurement time.

The mathematical operation of Fourier transformation is also inherent to the particle sizing technique because the measured diffraction patterns (the spatial distributions of light intensity) are proportional to the square of the Fourier transformation of the complex amplitude of the light in the sample region. However, the operation of finding the size distribution of the particle sample from the measured diffraction pattern can be reduced

to a straightforward multiplication of matrices. So, once an inverse matrix has been obtained, the process consists of measuring a diffraction pattern and multiplying this pattern by the inverted matrix. The inverted matrix remains constant and is calculated only once. The result of the multiplication is a set of numbers representing the size distribution of the particles in the sample. The matrix multiplication can be performed essentially in real-time.

A line drawing of the section of the optics directly involved in the production and measurement of the diffraction patterns is shown in Figure 1. A collimated laser beam illuminates the sample space. The light transmitted through the sample volume is transformed by the lens, and the Fraunhofer diffraction patterns are formed in the back focal plane of the lens. A detector array located in this plane measures the spatial distributions of irradiance in the diffraction patterns.

The diffraction pattern produced by a small circular aperture in an opaque screen in the front focal plane of the lenses is described by the following equation [1]:

$$I(r) = I_o \left[\frac{kd^2}{8f}\right]^2 \left[\frac{2J_1(krd/2f)}{krd/2f}\right]^2$$

where $I(r)$ is the diffraction pattern irradiance a distance r from the optic axis

I_o is the irradiance of the uniform incident beam

k is $2\pi/\lambda$, where λ is the wavelength of the laser radiation

d is the diameter of the circular aperture

f is the focal length of the lens

$J_1()$ is the first order Bessel function of first kind with argument $(krd/2f)$.

This pattern consists of a bright circular disk at the center (the Airy disk) surrounded by alternate dark and bright rings. The dark rings occur at the zeros of the Bessel function. The circular symmetry of the aperture is preserved in the diffraction pattern. The radii of the rings in the pattern can be described by:

$$r = \frac{mf\lambda}{d}$$

where the value of m is associated with the ring brightness as indicated in

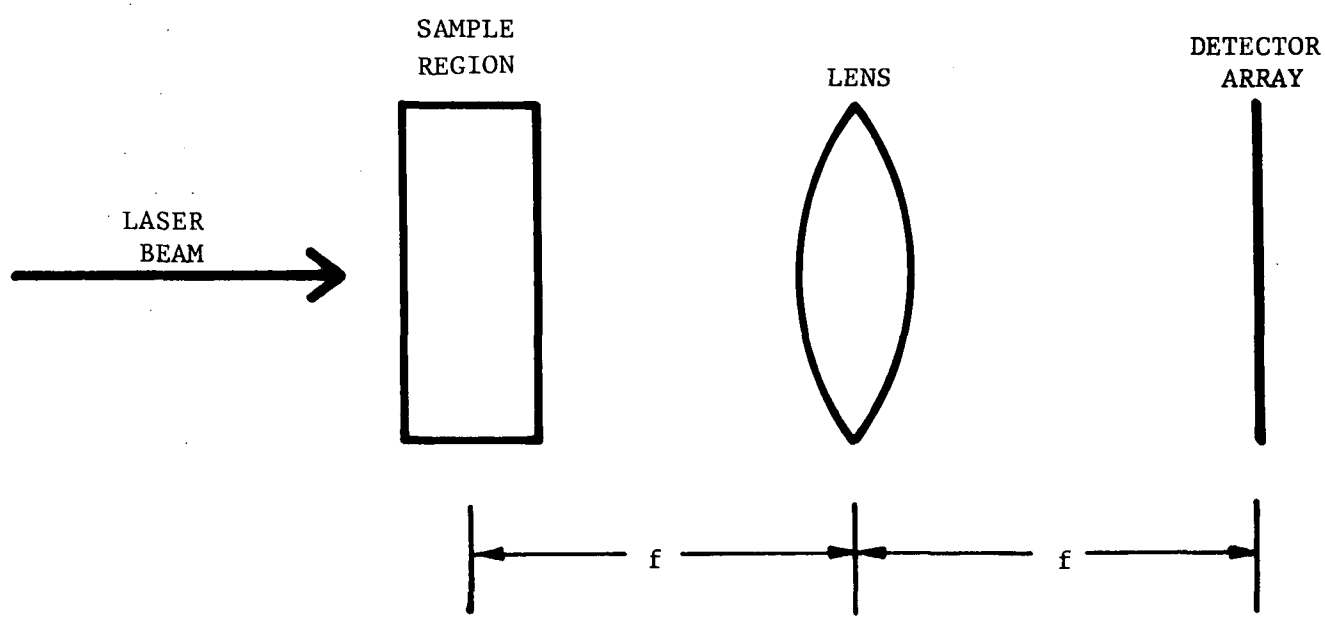

Figure 1. Basic Optical System for Producing and Measuring Diffraction Patterns.

Table 1 [2]. The values of m associated with the dark rings are derived from the zeros of the Bessel function. The values of m associated with the bright rings give the radii to the peak intensity regions.

The important functional relationships are the direct relation between the radius of a chosen ring and either the focal length of the lens or the wavelength of the radiant energy, and the inverse relation between the radius of the ring and the diameter of the aperture. An increase in either focal length or wavelength produces an increase in radius of the rings in the diffraction pattern; that is, the diffraction pattern is expanded. An increase in the aperture diameter compresses the size of the diffraction pattern.

The reason for beginning this discussion of the theory with the above description of the Fraunhofer diffraction pattern produced by a pinhole aperture in an opaque screen is that this case is discussed in most textbooks on optics and hence is most familiar. However, the simplest case of the actual problem of interest would consist of the complementary situation of an opaque circular disk in a transparent screen. By Babinet's principle we know that the diffraction patterns of complementary obstacles are the same, except near the point where the optic axis intercepts the pattern [3]. So the properties of the circular-aperture diffraction pattern apply as well to the patterns produced by spherical particles.

Also, from scattering theory we know that the scattering efficiency is two for spherical particles of radius much larger than the wavelength. The scattering efficiency is defined as the ratio of the total amount of light scattered to the amount of light incident on the geometrical cross-section of the particle. A scattering efficiency of two for large particles implies that the total light scattered by a spherical particle is twice the amount of light incident on the geometric cross section of the particle.

Another way of thinking of this is that the light directly incident on a large spherical particle and the light passing around the particle within a ring of area equal to the particle cross-section are both scattered. In the case of an opaque particle the light directly incident on the particle cross-section is either reflected or absorbed and only the light passing through the ring around the particle contributes to the particle diffraction pattern. But this amount of light is the same as that incident on a circular aperture of the same diameter as the particle. In the case of a circular aperture the light passing through the aperture produces the diffraction pattern. So, the total amount of light in the diffraction patterns produced by large, opaque particles of circular cross-section is the same as the amount of light in the diffraction pattern of a circular aperture in an opaque screen. By Babinet's principle we know that the two patterns are the same both in shape and irradiance.

TABLE 1

CIRCULAR APERTURE DIFFRACTION PATTERN PARAMETERS [2]

Diffraction Ring	m
1st Dark	1.220
2nd Bright	1.635
2nd Dark	2.233
3rd Bright	2.679
3rd Dark	3.238
4th Bright	3.699
4th Dark	4.241
5th Bright	4.710
5th Dark	5.243

Before going further we must point out a consideration that limits the minimum number of particles whose diffraction pattern can actually be measured with no more than the reasonable amount of precision available. The diffraction pattern of a pinhole in an opaque screen is relatively simple. Only the light that passes through the pinhole goes into the diffraction pattern and all of it is accounted for by the pattern. For the case of an opaque, spherical particle, however, there are actually two diffraction patterns present and superimposed. One is the pattern characteristic of the particle. The other pattern present is characteristic of a circular aperture whose diameter is the same as either the laser beam diameter or the entrance pupil diameter of the lens, whichever is smaller. The dimensions of this second pattern are greatly compressed in comparison with the pattern due to the particle because of the usually much larger effective diameter of the laser beam. Because of this compression the second diffraction pattern may be significant only in a negligibly small region at the optic axis, as indicated in the statement of Babinet's principle above. However, the irradiances in the two patterns must be compared as well as the geometrical dimensions. Practically all of the light in the laser beam goes into the diffraction pattern due to the limiting aperture. Only a relatively small portion of the light goes into the pattern characteristic of a single particle. In order to increase the irradiance in the particle diffraction pattern, a larger number of particles of the same size must be placed in the laser beam. The minimum number of particles of one size that produces a pattern distinguishable from the laser beam pattern determines the minimum number of particles of that size that can be resolved. Results of calculations based on these ideas will be presented later.

Another aspect of the diffraction pattern produced by a particle must now be discussed. This concerns the location of the particle in the laser beam. Light must be thought of as a complex quantity involving both amplitude and phase. However, the physical parameter that is actually measured is proportional to the square of the amplitude of the resultant of all the superimposed components. The phase information is not measured. When a single particle is moved in the sample plane, only the phase of the field vector is changed at any point in the diffraction pattern. The amplitude, and hence the irradiance, stays constant. Thus, there is no detectable change in the diffraction pattern when the particle is moved provided that the irradiance of the incident beam is uniform. This means that a particle fixed on a substrate will produce the same diffraction pattern as a particle falling through the laser beam. This is the justification for using permanent samples to simulate time-varying aerosol samples.

When two or more particles are in the beam simultaneously, the resultant amplitude in the diffraction pattern is a function of the phase of each component, and constructive and destructive interference effects may be observed. However, when the number of particles is very large and the positions of the particles are random, the irradiances rather than the

amplitudes of the diffraction patterns add linearly. Therefore, a random monodisperse sample of N particles would produce a diffraction pattern with N times the irradiance of a single particle.

If the sizes of the particles in a sample vary over a wide range, then the distinctive bright and dark circles in the diffraction pattern of a monodisperse sample become smeared and washed out. However, provided the measurements are made with adequate precision, the inversion process transforms the pattern into the size distribution of the particles that produced the pattern. The precision with which the diffraction measurements are made determines the particle size resolution achievable. This will be discussed in more detail later.

So far we have been discussing the diffraction patterns of opaque particles. If the particles are transparent then the refractive index is important in determining the shape of the diffraction pattern. The process can be thought of as consisting of a combination of diffraction and refraction. The light passing around the particle through a ring whose area is equal to the cross-sectional area of the particle produces the diffraction pattern we have been considering. The light transmitted through the particle is refracted at two surfaces and, since the phase relation between the diffracted and refracted components remains constant in time, interference will occur between the two components. If the amplitude of the transmitted light is comparable to that of the diffracted light, the interference will be significant. This occurs, for instance, in water droplets and is referred to as anomalous diffraction [4]. This effect can be accounted for in the diffraction pattern technique of particle sizing provided the refractive index of the particles is the same for all particles.

Particles of shapes other than spherical can produce dramatically different diffraction patterns. If the particles are all the same shape this effect may be at least partially compensated for in the inversion process, particularly if allowance is made for measuring the angular variation of the diffraction patterns as well as the radial variation.

The functional relation between the size-distribution of the particles in a sample and the diffraction pattern produced by that pattern can be written as an integral equation:

$$I(r) = \int_{a_1}^{a_2} n(a)\ G(r,a)\ da$$

where I(r) represents the irradiance at a ring of radius r in the diffraction pattern

a_1 is the radius of the smallest particle in the sample

a_2 is the radius of the largest particle in the sample

n(a) represents the number of particles per unit volume as a function of particle radius.

$$G(r,a) = I_o\left(\frac{ka^2}{f}\right)^2\left[\frac{J_1(kar/f)}{kar/f}\right]^2$$

is the kernel function of the integral equation. In this case, the kernel function is the expression for Fraunhofer diffraction by an aperture of radius a. The integral equation above is referred to as a Fredholm integral equation of the first kind. The variables whose values are known are the irradiance I(r) and the kernel function G(r,a). The unknown quantity is n(a), the size distribution of the particles producing the measured diffraction pattern.

Anderson and Beissner [5] have formulated the problem in matrix notation as follows:

$$I = GN$$

where I is a column matrix whose elements are the irradiance measurements at a set of radial distances.

G is a rectangular (in general not square) matrix whose elements are discrete values of the kernel function described earlier.

N is a column matrix whose elements are the number of particles as a function of size.

The solution of the above matrix equation for N, the discrete values of the particle size distribution, is [6]

$$N = (G^TG)^{-1}\ G^T\ I$$

where G^T is the transpose of G. This solution minimizes the sum of the squares of the errors.

The above solution will yield unstable results if the columns of G are almost linearly dependent. This will occur when the experimental error in

the diffraction pattern measurement is significant compared with the actual difference between diffraction patterns produced by particles differing in size by the resolution limit. This error limits the size-resolution achievable by the indirect method of particle sizing. The particle size intervals must be large enough to insure that the diffraction pattern produced by particles in adjacent intervals differ by quantities that are large compared with the experimental error in the irradiance measurements. If the error in the irradiance measurements is too large, one or more columns of G will be linear combinations of other columns of G. Under this condition G will not have a generalized inverse and there will not be a solution. When the columns of G are almost linearly dependent, small errors in the measured data cause large variations in the solution. When this is true the matrix is said to be ill-conditioned.

Twomey and Howell [7] have suggested a procedure for calculating the number of independent pieces of information available in the solution. It is based on an analysis of the eigenvalues associated with the covariance matrix of the kernel functions. For a given matrix G of kernel functions the covariance matrix is G^TG. For the diffraction pattern technique of particle size measurement the covariance matrix is positive, definite, and symmetric, but not well-conditioned.

The eigenvalues of the covariance matrix are calculated and placed in the order of decreasing values. These ordered eigenvalues are compared with a measure of the error in the experimental data. The number of eigenvalues above this measure is the number of independent inferences that can be drawn from the data with that level of error. So long as the number of measurements is larger than the number of independent inferences, the most direct way to increase the number of inferences is to increase the precision of the measurements rather than to increase the number of measurements.

SECTION II

SUMMARY

The work on this grant was directed toward the study of aerosol dynamics by applying a diffraction pattern analysis technique to the problem of measuring the size distribution of large particles in air. The technique consisted of deriving a transformation matrix which was used to convert measured diffraction patterns to the size distribution of the samples that produced the patterns. The greatest success achieved was in the measurement of the size distribution of an array of circular apertures in an opaque background. The more difficult case, that of analyzing the diffraction pattern produced by an array of particles in a transparent medium, yielded only moderate success. The use of a better quality detector array and lens would improve the results, but the technique will probably be limited to particle samples of large number densities.

SECTION III

CONCLUSIONS

This report presents the results of an application of diffraction pattern analysis to the measurement of the number and size of large particles in air. The conclusions drawn from the results of this effort are presented below.

(1) A diffraction pattern inversion technique for sizing particles was demonstrated successfully for a polydisperse array of circular apertures in an opaque background.

(2) This technique appears to be best suited to the problem of counting and sizing apertures in opaque materials.

(3) Extension of the technique to the problem of sizing particles in air appears to be feasible for samples of large number density.

(4) This technique may be applicable to the problem of monitoring the particulate emissions as a function of size from industrial smokestacks. The advantages of this inversion technique are the large sample volume and the real-time output of the size distribution.

(5) The literature search done in conjunction with the work reported here indicated that the inversion process has been applied to a wide variety of problems in the areas of remote sensing, spectroscopy, geology, and particle sizing.

SECTION IV

RECOMMENDATIONS

The further development of the technique described in this report should consist of the following steps:

(1) Design a computer simulation of the application based on the results indicated in this report. Include a complete eigenvalue analysis as described by Twomey and Howell [7].

(2) Design and purchase a detector array and transform lens optimized for the application. Two important modifications to the RSI array would consist of antireflection coating the face of the detector and drilling a hole through the center element to allow the intense "dc component" to pass through without being reflected between the detector and the transform lens.

(3) A minicomputer should be used to take and process the data from the detector array.

(4) Modify the computer program for accurately simulating diffraction patterns from both apertures and particles by including correction factors to account for the observed detector performance.

(5) Verify the accuracy by comparing computer generated and experimentally measured patterns.

(6) Generate an inversion matrix from accurately computed patterns for monodisperse samples.

(7) Measure the diffraction patterns from known polydisperse samples and apply the inversion matrix in order to compare the measured and the known values.

SECTION V

EXPERIMENTAL PLAN

The main phases of this project consisted of:

A. Modification of computer programs for simulating the technique and inverting data.

B. Analysis of the diffraction patterns from single pinholes in metal disks.

C. Analysis of the diffraction patterns from arrays of circular apertures and opaque spots on photographic transparencies.

D. Analysis of the diffraction patterns from actual particle samples on microscope slides.

E. Analysis of the diffraction patterns from actual aerosol samples.

Each of these phases will be discussed briefly now, and in more detail in Section VI.

A. Three main computer programs were utilized. The first program, labelled POWER, calculated the diffraction pattern data to be measured by a detector with the geometry of our Recognition Systems, Inc. (RSI) array. Parameters in this program are the particle diameter, transform lens focal length, and laser wavelength. The output consisted of sets of numbers proportional to the expected output of the RSI array, one set of 31 values for each particle diameter. Each of the 31 values in a set corresponded to the output of one of the 31 ring elements concentric with the center element of the RSI array. This was the starting point for a computer simulation of the particle sizing technique.

The second program was one that utilized diffraction pattern data to calculate the inversion matrix. This matrix was then used to transform an arbitrary diffraction pattern to the size distribution of the sample that produced the pattern. The diffraction pattern could be either computer-generated or actual data. This program also calculated the eigenvalues and eigenvectors of the covariance matrix. A "smoothing function" [8] was included in order to provide a controlled amount of smoothing to oscillating solutions in the case of an ill-conditioned matrix.

The third program performed a matrix multiplication between the previously calculated inversion matrix and any set of diffraction pattern data. The

result of this multiplication was a measure of the size distribution of the particle sample that produced the diffraction pattern. Both the inversion matrix and the diffraction data could be either computer generated or actual measured data. This flexibility was used to provide pure computer simulation with noise-free data, a measure of the effect of error in either the inversion matrix or the diffraction pattern data, and a comparison between results obtained by a pure simulation and a completely experimental set of data.

B. The second phase of the project consisted of measuring and analyzing the diffraction patterns from single pinholes in metal disks. The reason for doing this was that it provided us with experimental data under nearly ideal conditions. The experimental data differ from the computer generated diffraction patterns both in precision (the number of significant digits) and accuracy. The conditions were regarded as ideal in comparison with an experimental measure of the diffraction patterns of actual particles in that only the diffraction pattern characteristic of the pinhole diameter was present. As pointed out earlier the diffraction pattern due to an aerosol sample has superimposed on it the diffraction pattern due to the laser beam diameter.

C. The third phase of this project consisted of measuring and analyzing the diffraction patterns from arrays of circular apertures and opaque spots on photographic transparencies. This was one step closer to the actual problem of measuring the patterns produced by aerosol samples, but it also provided a technique for generating permanent, monodisperse samples.

D. The fourth phase of this project consisted of measuring and analyzing the diffraction patterns of samples of particles deposited on microscope slides. Again, this was one step closer to the goal of measuring aerosol samples, and yet it provided the convenience of fairly permanent samples that could be examined under a microscope.

E. The fifth phase of this project consisted of measuring and analyzing the diffraction patterns of actual aerosol samples. This was the goal of the project to which the previous phases were directed.

SECTION VI

METHODS, PROCEDURES, RESULTS, AND DISCUSSIONS

Figure 1 in the discussion of the theory illustrated only the Fourier transform lens segment of the complete optical system. Figure 2 shows the complete system as normally used on this project. The argon ion laser was a Coherent Radiation Model 53 capable of producing about 1.5 W at a wavelength of 488 nm. The laser output was focused on a pinhole filter to eliminate undesired components and then allowed to expand to a diameter of 50 mm before being recollimated.

The irradiance of the pinhole filter/collimator was found to fluctuate even though the laser had a built-in light sampling and controlling system. The internal sampling was replaced by an external detector and amplifiers in the form of a United Detector Technology (UDT) Model 40A radiometer. The output of the radiometer amplifier was fed into the laser power supply control circuit to close the control loop.

Only the 3 mm diameter center segment of the 50 mm diameter expanded beam was passed by the aperture of the beam expander. This was done to insure uniformity of the irradiance across the beam in the sample region and to minimize the amount of unnecessary light on the detector. Most of the work was done with a Fourier transform lens sold by Tropel, Inc. This lens was supposedly designed to be used at a wavelength of 488 nm corresponding to one of the lines emitted by the argon-ion laser. The effective focal length (EFL) of the lens is 59.89 cm, and the diameter of the entrance pupil is 58.4 mm. The overall transmission through the 6-element lens is supposed to be greater than 99% at 488 nm. However, the measured transmission turned out to be only about 82%. Unfortunately, the 17% difference appears to be due largely to reflection at each air-glass interface even though the elements are anti-reflection (AR) coated. A portion of the internally reflected light is superimposed on the diffraction pattern to be measured at the detector array. This reduced the accuracy and also the usefulness of the Tropel lens. Photographic and television lenses were also used with good results when shorter focal lengths were required.

When there were no samples in the laser beam, the light in the beam was focused at the center of the detector array. If the undiffracted light were allowed to impinge upon the face of the detector, a portion of it would be reflected back toward the lens. Because of the relatively high reflection from the lens surfaces some of the light would be reflected toward the detector again. In order to reduce this component of the reflected light, an optical filter was used to trap the undiffracted light and guide it away from the detector region.

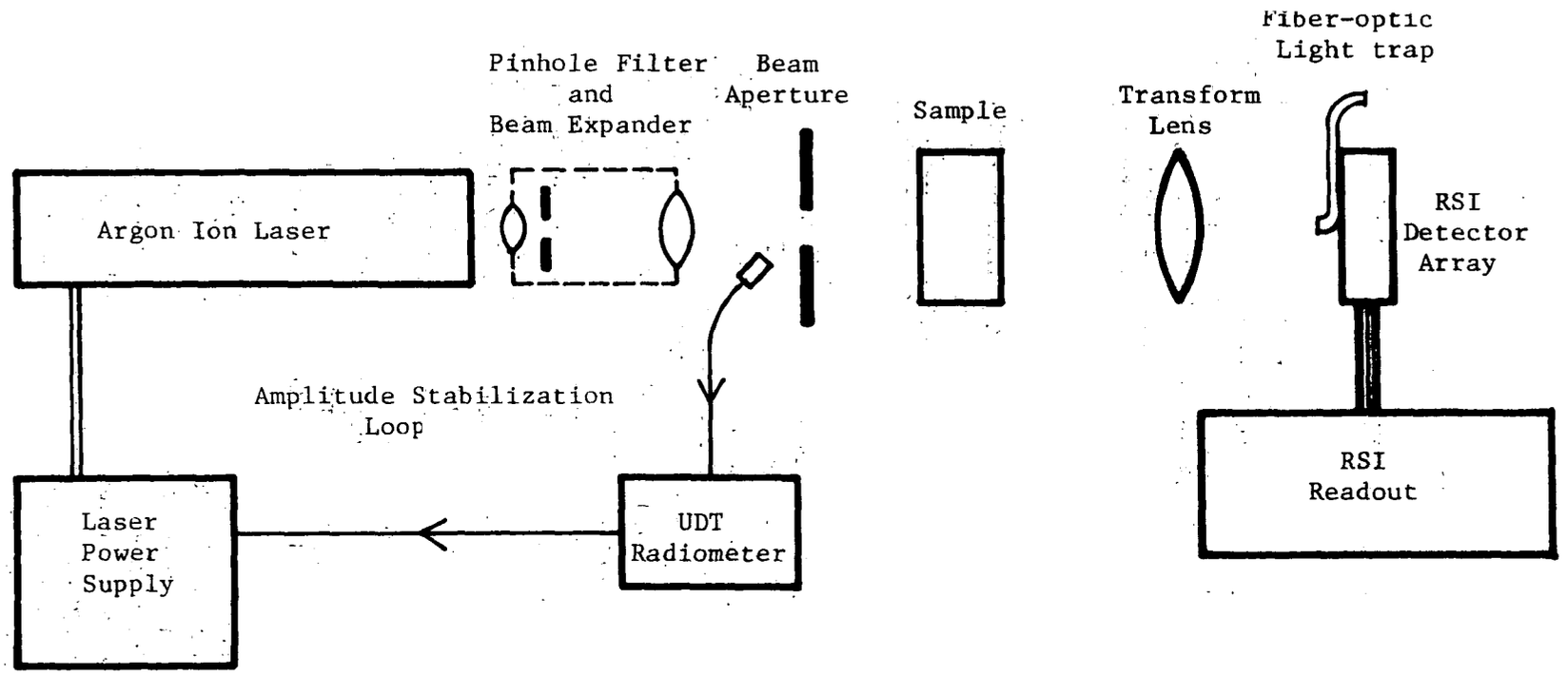

Figure 2. Complete Diffraction Pattern Particle Sizing System.

The detector array that was used to measure the majority of the diffraction patterns was a Recognition Systems, Inc. diffraction pattern sampling unit. The geometry of the detector array is such that one half of the 3.18 cm diameter circular area is covered by 31 concentric ring elements and 1 center element. The other half is covered by 32 wedge shaped elements. The signal output of the ring elements was proportional to the integral of the irradiance in the diffraction pattern over the area of each element. The ideal detector geometry for circularly symmetric diffraction patterns would consist of concentric rings that integrated around a full 360° circle rather than the 160° almost-half-rings of the RSI array. However, the difference is probably not significant in comparison with the potential improvement from other possible modifications. These ideas were discussed under RECOMMENDATIONS.

Another detector array that became available for a short time during the fourth and fifth phases of this project was a fiber-optic/photodiode-array built at Georgia Tech for NASA [9]. This consisted of an array of 90,000 optical fibers of 76 μm diameter arranged at one end in 168 rings concentric with the center fiber. At the other end of the 60 cm long fiber bundle each ring of fibers was terminated with a PIN photodiode. The fibers collected the light from concentric circles and guided it to individual photodetectors for each circle. The photodiodes produced signals proportional to the integral of the irradiance over each circle. The output of the array of 169 photodiodes was electronically scanned, digitized, and fed into a minicomputer. This provided much faster accumulation of data and allowed real-time subtraction of background levels from the signal-plus-background levels to yield signals proportional to the irradiances in the particle diffraction patterns. These diffraction patterns were displayed in real-time which provided immediate feedback concerning the results of any sample changes or system adjustments.

As was indicated in Section V the first phase of this project consisted of modifying the computer programs that had been used at Georgia Tech for earlier work on this particle sizing technique. The first program modified for this project was one labelled POWER. This program calculated values proportional to the power (integrated over the area) incident on each photodetector in a diffraction pattern. The flux density (power/area) at a radius r in the Fraunhofer diffraction pattern of a uniformly illuminated circular aperture is:

$$I(r) = I_o \left[\frac{kd^2}{8f}\right]^2 \left[\frac{2J_1(krd/2f)}{\frac{krd}{2f}}\right]^2$$

where I_o is the uniform flux density (power/area) incident on the aperture. The units of $I(r)$ are determined by the units in which I_o is given.

$k = 2\pi/\lambda$ where λ is the wavelength of the radiant energy

d = diameter of the aperture

f = effective focal length of the transform lens

$J_1()$ = first order Bessel function of the first kind.

r = radial distance in the plane of the diffraction pattern from the optic axis. The center of the diffraction pattern occurs at the optic axis of the transform lens independent of the location of the aperture with respect to the optic axis.

The flux density was integrated over the area of each detector element in order to obtain a value proportional to the signal out of each element. The proportionality constant was the responsivity (voltage/power) of the detector element. The total flux or power incident on detector element N is indicated as

$$P(N) = \int_{r_{N,min}}^{r_{N,max}} I(r)\, dA$$

where $r_{N,max}$ = radial distance to outer edge of ring element N

$r_{N,min}$ = radial distance to inner edge of ring element N

dA = infinitesimal element of area.

The geometry of the ring elements of the RSI detector array was such that the rings subtended an angle of only 160° at the center of the array. The infinitesimal area elements in the above integration were taken as strips of length equal to the arc formed by the detector and thickness equal to dr:

$$dA = \frac{160}{180}\, \pi r\, dr.$$

Substituting for $I(r)$ and dA, the expression for the power in ring N became:

$$P(N) = \frac{2(\pi d)^4 I_o}{9\pi(f\lambda)^2} \int_{r_{N,\,min}}^{r_{N,\,max}} r \left[\frac{J_1\left(\frac{\pi r d}{f\lambda}\right)}{\frac{\pi r d}{f\lambda}} \right]^2 dr.$$

The constant I_o was set equal to 1 in the computer program. Because the dimensions of d, f, and r were converted to microns in the computer program, the values of power calculated by the program must be multiplied by 10^{-8} to yield the power in milliwatts for an incident irradiance in the laser beam of 1 mW/cm^2.

In the earlier discussion of the mathematics of the diffraction pattern-to-particle size distribution transformation, we indicated that the transformation matrix was

$$W = (G^T G)^{-1} G^T.$$

This is the least-squares solution for N of the matrix equation

$$GN = I.$$

That is, $N = WI = (G^T G)^{-1} G^T I$.

A somewhat more sophisticated solution which includes a parameter for smoothing oscillations in the solution for an ill-conditioned matrix is given by [8]

$$W = U(\Lambda + \gamma I)^{-1} U^T$$

where W is the "inversion matrix" which can be used to multiply a set of diffraction pattern data to obtain the size distribution of the particles that produced the diffraction pattern.

U is the matrix whose columns are the eigenvectors of the $G^T G$ matrix ordered to correspond to the eigenvalues in descending order.

Λ is the elementary matrix of ordered eigenvalues on the diagonal and zeros in all other positions.

γ is the value of the smoothing parameter.

I is the identity matrix of the same order as Λ.

U^T is the transpose of U.

The program SMLS calculated the above SMoothed Least Squares solution. First it allowed the columns of G to be weighted by any distribution function. This was done in order to test the effect of normalizing the columns of G such that the diagonal elements of G^TG were unity. The program then calculated the eigenvalues and eigenvectors of G^TG and then ordered both the eigenvalues and eigenvectors in the order of decreasing eigenvalues. The smoothing parameters were usually set to zero in this project. This had the effect of reducing the solution to the simpler form:

$$W = (G^T G)^{-1} G^T.$$

It was felt that at this stage unsmoothed solutions could be compared more meaningfully than solutions with various amounts of smoothing. The results were always tested by multiplying the sum of the columns of G by the inversion matrix to see if the result was the sum of the size distributions used to calculate G.

The DIST program calculated size distributions by multiplying columns of diffraction pattern data by an inversion matrix calculated by the SMLS program. The sets of calculated diffraction pattern data were summed and then inverted. In this way sets of diffraction patterns from known monodisperse samples were read in and summed. The result of the matrix multiplication was compared to the sum of the known distribution of the data entered. This was done primarily in testing computer simulations of particle sizing experiments. Sets of measured diffraction pattern data were entered one column at a time and not summed with other data before being inverted. The results were then compared with the particle size distribution if it was known. This was done to simplify the comparison between the inversion results and the relatively poorly known size distributions.

In order to perform a computer simulation of the technique for particle sizing by diffraction pattern analysis, the first step was the selection of a set of particle size intervals. This was done by applying one of several criteria relating the geometry of the photodetector array with the characteristics of the diffraction patterns produced with 0.488 μm wavelength light and a transform lens of 59.89 cm focal length. These particle sizes were then used in conjunction with the computer program labeled POWER to generate the data for calculating an inversion matrix.

In the process of calculating an inversion matrix, as was indicated earlier, the eigenvalues of the covariance matrix were calculated. Based on the

paper of Twomey and Howell [7] the range of the eigenvalues was used as a measure of the success in the selection of the particle size intervals. A wide range of values (usually covering several decades) indicated a degree of dependence among the basis set of diffraction patterns associated with the set of particle sizes. This implied that within the limits of experimental error at least one of the diffraction patterns could be approximated by a linear combination of the other patterns. When this condition occurred the matrix inversion yielded an unstable or worthless solution.

The various criteria that have been tried will first be described. Then the results of the eigenvalue analysis will be presented and compared. The following criteria were tested and will be described here:

A. First diffraction minimum at successive detector rings.
B. Successive diffraction nulls and antinulls at detector ring number 32.
C. Metal pinhole sizes available.
D. Equally spaced particle diameters.
E. Equally spaced diffraction peaks.
F. Diffraction pattern intersections at 95% of peak.
G. Diffraction peak at first null of next larger size.

A. First diffraction minimum at successive detector rings.

This criterion was the most overly optimistic in terms of the expected resolution. The idea was based on the fact that if the position of the first null were known, then the diameter of the particle could be calculated from

$$d = \frac{mf\lambda}{r}$$

where m = 1.220 for the first null

f = focal length of lens

λ = wavelength of light

r = radial distance from optic axis to first null.

Particles could easily be sized one at a time by this criterion with a resolution determined primarily by the spacing between adjacent detector elements. The particle sizes resulting from the application of this criterion are listed in Table 2 along with the detector ring number and radius at which the first null occurred.

TABLE 2

PARTICLE SIZES FOR WHICH THE FIRST MINIMUM IN THE DIFFRACTION PATTERNS OCCURRED AT SUCCESSIVE DETECTOR RINGS

Particle Diameter (μm)	Ring Number	Average Radius (mm)
23.02	32	15.48
24.32	31	14.66
25.75	30	13.85
27.30	29	13.06
29.02	28	12.29
30.90	27	11.54
32.96	26	10.82
35.24	25	10.12
37.78	24	9.44
40.55	23	8.78
43.71	22	8.15
47.27	21	7.53
51.39	20	6.94
55.98	19	6.37
61.25	18	5.82
67.33	17	5.30
74.40	16	4.79
82.68	15	4.32
92.48	14	3.86
104.24	13	3.42

This set of particle sizes ranged from 23 to 104 μm diameter. Either the lens focal length or the laser wavelength could be changed to cover the range from 5 to 100 μm diameter. For instance, a lens of 13.0 cm focal length would extend the size range down to 5 μm diameter particles. However, it was decided that all the preliminary work would be performed with the 59.89 cm focal length Tropel lens at the 0.488 μm wavelength. Under these conditions the 23 to 104 μm particle range was divided into 20 subintervals with the greatest resolution at the small end of the range.

It should be noted that the particle sizes tabulated corresponded to the particle size at the center of each subinterval. The upper and lower limits of each subinterval were not calculated in most cases.

The most interesting data associated with this set of particle sizes are the set of ordered eigenvalues associated with the covariance matrix G^TG of the diffraction patterns. This set of eigenvalues is listed in Table 3. Note that the computer format for indicating powers of 10 is used, e.g. $1.74 + 6 \equiv 1.74 \times 10^6$.

TABLE 3

ORDERED EIGENVALUES OF COVARIANCE MATRIX
OBTAINED FROM THE FIRST CRITERION

1	1.74 + 6
2	1.25 + 5
3	2.66 + 4
4	8.87 + 3
5	3.70 + 3
6	1.79 + 3
7	9.44 + 2
8	5.28 + 2
9	2.78 + 2
10	5.79 + 1
11	1.15 + 1
12	2.41 - 2
13	9.14 - 5
14	2.75 - 5
15	1.16 - 5
16	4.34 - 6
17	1.97 - 6
18	6.72 - 7
19	2.09 - 7
20	6.52 - 8

The range of the eigenvalues covered about 14 decades. The implication of this was that the hoped for resolution of 20 subintervals is much too fine. The diffraction patterns characteristic of the 20 particle sizes were not sufficiently independent to yield a meaningful solution.

B. Successive diffraction pattern nulls and antinulls at the outermost detector element.

The outermost ring element of the detector array was labeled ring #32. The criterion discussed here is somewhat analogous to the resolution criterion of Fourier transform spectroscopy and was studied for this reason. Table 4 lists the particle diameters that satisfy this criterion.

TABLE 4

PARTICLE SIZES FOR WHICH SUCCESSIVE DIFFRACTION PATTERN MINIMA AND MAXIMA OCCURRED AT DETECTOR RING 32

Condition at Ring #32	Particle Diameter (μm)
1st min.	23.0
2nd max.	30.8
2nd min.	42.1
3rd max.	50.5
3rd min.	61.1
4th max.	69.8
4th min.	80.0
5th max.	88.9
5th min.	98.9

Several things should be noted from the data in Table 4. This criterion yielded a more uniform spacing between subintervals than did the first criterion. Also, there are now only 9 subintervals spanning the size range from 22 to 98.8 μm diameter. The particle diameters listed here were selected from the results of the computer program POWER in which the diffraction patterns to be measured by the RSI array were simulated.

The results of the eigenvalue analysis are listed in Table 5.

TABLE 5

ORDERED EIGENVALUES OF COVARIANCE MATRIX OBTAINED FROM THE SECOND CRITERION

Order Number	Eigenvalue
1	1.32 + 6
2	6.25 + 4
3	1.15 + 4
4	3.81 + 3
5	1.42 + 3
6	8.02 + 2
7	4.19 + 2
8	2.17 + 2
9	7.43 + 1

The eigenvalues in Table 5 range over only about five decades rather than the 14 decades indicated in the results for the first criterion. Even though this was a significant improvement it still indicated probable difficulty in obtaining meaningful data from the inversion of experimental data.

C. Metal Pinhole Sizes Available

This third "criterion" was used just as a comparison with the other criteria that were based on physical reasoning. The set of pinhole diameters is listed in Table 6. This set of six pinholes spanned the range from 25 to 76 μm diameter. These sizes were comparable to the first seven sizes selected by the second criterion except for the absence of a pinhole near 42.1 μm diameter.

TABLE 6

METAL PINHOLE DIAMETERS AND THE ORDERED EIGENVALUES OF THE COVARIANCE MATRIX

(μm)	Ordered Eigenvalues
25	5.21 + 3
29	2.41 + 2
52	1.83 + 1
62	3.07 + 0
68	8.47 - 1
76	1.65 - 1

The ordered eigenvalues for this set of particle sizes is also listed in Table 6. It is seen that the rate of decrease in the eigenvalue is comparable for the two cases. This was not too surprising because the particle sizes were similar.

D. Uniformly spaced particle diameters

This criterion, like the one just preceding, was not based on any likely principle. It was selected as a matter of convenience to allow a comparison of the results of the analysis of the ordered eigenvalues. The selected particle diameters are listed in Table 7. The ordered eigenvalues of the covariance matrix associated with this set of particle sizes are also listed in Table 7. The range of the eigenvalues was still too large to be acceptable.

TABLE 7

UNIFORMLY SPACED APERTURE DIAMETERS AND THE ASSOCIATED ORDERED EIGENVALUES

Particle Diameter (μm)	Ordered Eigenvalues
10.0	4.27 + 5
20.0	2.03 + 4
30.0	3.66 + 3
40.0	1.17 + 3
50.0	4.88 + 2
60.0	2.27 + 2
70.0	8.20 + 1
80.0	3.27 + 0

E. Equally Spaced Diffraction Peaks

This criterion was applied by selecting particle diameters that produced diffraction pattern maxima at detector rings numbered 32, 29, 26, 23, 20, 17, 14, 11, and 8. The resultant particle sizes are listed in Table 8.

TABLE 8

PARTICLE DIAMETERS FOR UNIFORMLY SPACED DIFFRACTION MAXIMA AND THE ASSOCIATED ORDERED EIGENVALUES

Detector Ring Number	Avg. Radius (mm)	Particle Diameter (μm)	Ordered Eigenvalues
32	15.5	9.5	4.91 + 5
29	13.1	11.5	2.34 + 4
26	10.8	14.0	2.57 + 3
23	8.8	17.5	2.55 + 2
20	6.9	22.0	1.36 + 2
17	5.3	29.0	1.62 + 1
14	3.9	40.0	2.17 - 2
11	2.6	55.0	1.21 - 6
8	1.6	94.0	3.60 - 12

The results of calculating the eigenvalues associated with these particle sizes are also shown in Table 8. It is seen that the eigenvalues span about 17 decades, an enormous range. There was about one decade difference between adjacent eigenvalues for the first six. Then the values dropped off rapidly. This indicated that a better selection would have consisted of the set of six particle sizes that produced diffraction maxima at uniformly spaced detector ring numbers on 32, 27, 22, 17, 12 and 7.

This set would have spanned about the same particle size range (9.5 - 100 μm) with the advantage of less overlap of the diffraction patterns due to adjacent particle sizes. This reduction of the attempted particle size resolution would have yielded a set of eigenvalues that covered a much smaller range because the diffraction patterns would have been more nearly independent.

One idea that was tried was to normalize the matrix of diffraction patterns such that the product of G transpose and G had one's along the main diagonal. In other words the dot product of each diffraction pattern with itself was set equal to one by multiplying each diffraction pattern by a suitable constant. This was done in order to make the diffraction patterns of the smaller particles comparable with those of the larger particles. However, this was accomplished by sacrificing particle-number resolution for the smaller particles especially. It was felt that a trade-off of particle-number resolution for particle-size resolution might be justified in many applications of this technique.

The normalization constants, the particle diameters and the ordered eigenvalues are listed in Table 9. The effect on the range of the eigenvalues has been somewhat beneficial indicating that it should be easier to classify particles according to the sizes indicated provided the number density of smaller particles was greater than that of larger particles in order to compensate for the less intense diffraction pattern produced by small particles. This sort of distribution is characteristic of many actual samples.

TABLE 9

RESULTS OF NORMALIZATION OF THE UNIFORMLY SPACED DIFFRACTION PATTERNS

Normalization Constant	Particle Diameter (μm)	Ordered Eigenvalues
3.25 - 1	9.5	6.03 + 0
1.81 - 1	11.5	1.96 + 0
1.06 - 1	14.0	6.50 - 1
6.21 - 2	17.5	2.49 - 1
3.74 - 2	22.0	7.71 - 2
2.03 - 2	29.0	2.79 - 2
9.89 - 3	40.0	1.51 - 4
4.86 - 3	55.0	2.00 - 8
1.47 - 3	94.0	1.97 - 10

F. Diffraction pattern intersections at 95% of peak

This criterion was applied by finding the largest particle diameter such that the maximum value of the detector output occurred at the detector ring furthest from the optic axis (ring #32). This condition was met by the 9.5 μm diameter particle when the Tropel lens was used at the 488 nm argon laser line. Note that because of the detector geometry (area of ring elements increased with ring number or distance from optic axis) particles of any diameter less than 9.5 μm yield measured diffraction patterns of very similar shape. The predominant change occurs in the intensity of the pattern, rather than the shape, when the particle diameter is varied from 0 to 9.5 μm. Since the intensity data were used to calculate the number of particles in a specific size range and the intensity was a very strong function of particle size in this range, the number calculated for this range by the inversion process was not unique. That is, essentially the same pattern would be produced by a very large number of submicron particles as by a much smaller number of

larger particles less than 9.5 μm diameter. Therefore the results in the smallest particle size interval obtained by the inversion process should be ignored.

The ring number at which the measured diffraction pattern was 95% of the value at ring #32 was then found. This was ring #29 for this lens, wavelength, and detector. Next a larger particle diameter was selected such that at ring #29 its measured diffraction pattern was about 95% of its peak value. A particle diameter of 14 μm satisfied this criterion. Continuing in this fashion, the set of seven particle diameters listed in Table 10 was selected.

TABLE 10

RESULTS OF THE SIXTH CRITERION

Particle Diameter (μm)	Ordered Eigenvalues
9.5	3.17 + 5
14	1.66 + 4
20	2.18 + 3
28	3.77 + 2
38	8.52 + 1
54	5.42 + 0
84	1.01 - 3

The ordered eigenvalues associated with the covariance matrix produced by the diffraction patterns of those particles is also listed. It is noted that the first six eigenvalues differed by about one order of magnitude between adjacent eigenvalues. However, the seventh eigenvalue was about three orders of magnitude smaller than the sixth. This indicated that the desired particle size resolution was probably too fine and that the size range from 9.5 to 84 μm diameter can actually be resolved into only six subintervals rather than the attempted seven.

The normalization procedure described under the preceding criteria was applied to this case also. The normalization constants and the resulting ordered eigenvalues are listed in Table 11.

TABLE 11

RESULTS OF NORMALIZATION ON THE SIXTH CRITERION

Particle Diameter (μm)	Normalization Constant	Ordered Eigenvalues
9.5	3.25 - 1	4.00 + 0
20.0	4.61 - 2	1.24 + 0
28.0	2.19 - 2	4.90 - 1
38.0	1.11 - 2	1.87 - 1
54.0	5.07 - 3	6.73 - 2
84.4	1.87 - 3	1.67 - 2

Also, it should be noted that the diffraction pattern for the 14.0 μm diameter particle was omitted from the basis set. This was done to remove the linear dependence indicated by the previous eigenvalue analysis. The 14.0 μm diameter particle was selected for removal on the basis of the results of forming the covariance matrix of the full set. This set of ordered eigenvalues was the most nearly uniform obtained to date. The implication is that this is probably a valid criterion for selecting the basis sets of particle sizes.

G. Diffraction peak at first null of next larger size.

This criterion is analogous to Rayleigh's criterion for diffraction-limited resolution. The basis for its consideration was the fact that the inner product of diffraction patterns for adjacent size intervals might be minimized by the fact that at the peak of one pattern the pattern for the next larger particle interval was zero. However, application of this pattern led to selection of the following particle sizes:

9.5 μm diam. - peak @ ring #32

23.0 μm diam. - 1st null @ ring #32
pk @ approximately #19.4

54 μm diam. - 1st null @ 19.4
pk @ #11.3

129 μm diam. - 1st null @ #11.3

Even if this set of basis sizes yielded a favorable set of eigenvalues we have already achieved better particle size resolution with the set of six particle sizes derived in the preceding criterion. A set of only

four particle sizes that spans a larger range is not as useful. The set of eigenvalues for this set of particle sizes was therefore not analyzed.

A set of pinhole apertures was purchased from Optimation, Inc. These apertures are centered in 9.5 mm diameter 300 series stainless steel discs. Table 12 lists the nominal and measured sizes of the apertures purchased.

A scanning electron microscope was used to measure the diameters of the apertures 35 μm and smaller. These measurements were made from photographs of the magnified images produced by the electron microscope at a known magnification. The magnification was measured by comparing the image size of a known grid pattern with the dimensions of the original. The 1 and 2.5 μm diameter apertures were not measured because they were not needed and because the difficulty of finding the aperture increased as the diameter decreased.

TABLE 12

SPECIFIED AND MEASURED METAL PINHOLE DIAMETERS

Nominal Diameter (μm)	Measured Diameter (μm)
1	-
2.5	-
5	5.2
7.5	7.6
10	9.8
12.5	12
15	14
17.5	18
25	25
35	29
50	52
60	62
70	68
80	76
90	84
100	104
200	184
300	295
400	377
500	507
600	598
700	684
800	769
900	916
1,000	1,000

The apertures 50 μm and larger in diameter were measured with a traveling microscope. These sizes were large enough that the measurement error was only a small part of the measured diameters.

The majority of the computer simulation experiments had been done assuming ideal conditions and precise data. The diffraction patterns produced by the metal pinhole apertures were measured primarily to obtain experience with the apparatus under the simplest conditions and to obtain data that contained actual measurement error.

The irradiance of the beam had to be high in order to obtain a measurable diffraction pattern particularly for the smallest apertures. This was achieved by using the beam from the laser as was, without filtering and expansion. The illuminated aperture was located in the entrance plane of the Tropel Fourier transform lens.

The diffraction patterns of the nominally 10, 25, 35, 50, 60, 70, 80 and 90 μm diameter apertures were measured by manually selecting the ring-elements in the RSI array and recording the signal levels indicated.

The results of calculating the aperture sizes from the measured diffraction patterns are indicated in Table 13. These calculations were based on the relation between the radii of the diffraction minima and the laser wavelength, lens focal length, and the aperture diameter. This relation is represented by the expression:

$$d = \frac{mf\lambda}{r}$$

where d is the aperture diameter

m = 1.220 for 1st minima
2.233 for 2nd minima
3.238 for 3rd minima

f = lens focal length

λ = wavelength of light used

r = radial distance from the optic axis to the diffraction minima, measured in the plane of the diffraction pattern.

The focal length was that of the Tropel Fourier transform lens, 59.89 cm. The wavelength was 0.488 μm for the light from the argon-ion laser.

The blanks in the data Table indicate that those diffraction minima were located beyond the RSI detector array and were not measured. The average values were calculated from the one, two or three diameters indicated and were rounded for presentation in the Table. These averages should be compared with the microscope measurements indicated in the next column. The agreement is good in general and could be improved with greater effort if that were required. The fact that the nominally 70 and 80 μm diameter apertures yielded the same results is due in part to the coarseness of the diffraction pattern sampling. This was determined by the geometry of the detector array.

TABLE 13

METAL PINHOLE DIAMETERS MEASURED BY LOCATION OF DIFFRACTION MINIMA

Nominal Aperture Diameter (μm)	Diameter Calculated from Position of 1st Minimum	2nd Minimum	3rd Minimum	Average	Microscope Measurement
25	24.3	-	-	24.3	25
35	29.0	-	-	29.0	29
50	43.8	44.5	-	44.2	52
60	56.0	56.5	-	56.3	62
70	74.4	74.3	72.5	73.7	68
80	74.4	74.3	72.5	73.7	76
90	82.6	80.1	82.0	81.6	84

Four sets of measured diffraction patterns from the set of metal pinhole apertures in the nominal size range from 10 through 90 μm diameter were averaged together before the inversion matrix and eigenvalues were calculated. The sizes of the apertures and the ordered eigenvalues are indicated in Table 14. It should be remembered that each eigenvalue is characteristic of the whole set of diffraction patterns. So, even though the eigenvalues are listed next to the aperture diameters it cannot be said that any one eigenvalue is associated with any one aperture size. In other words, if only one aperture size is changed the values of all the eigenvalues will be changed, in general. The only direct association between the aperture diameters and the eigenvalues is that the number of each is the same.

From Table 14 it is seen that there was a difference of almost two decades between the largest and next largest eigenvalues. The difference between adjacent eigenvalues then dropped off to less than one decade until the last two values. Here the change increased to about one decade between adjacent values. These results should be compared with those described earlier for the computer simulation testing of the various criteria applied to the selection of the particle size intervals. The normalization procedure also described above was not applied when these results were obtained.

Table 15 shows the results of normalizing the input data so that the inner product of each diffraction pattern with itself was unity. This improved the uniformity of the eigenvalues, but it made the apparent particle-number resolution worse, especially for the smaller particles. This is the same trade-off described earlier when the normalization procedure was introduced.

TABLE 14

EXPERIMENTAL RESULTS FROM METAL PINHOLES

Pinhole Diameter Nominal (μm)	Measured (μm)	Ordered Eigenvalues
10	9.8	2.44 + 3
25	25	7.63 + 1
35	29	1.70 + 1
50	52	1.26 + 1
60	62	5.01 + 0
70	68	2.44 + 0
80	76	2.65 - 1
90	84	3.54 - 2

TABLE 15

RESULTS FROM NORMALIZED EXPERIMENTAL DATA

Ordered Eigenvalues	
Before Normalization	After Normalization
2.44 + 3	5.83 + 0
7.63 + 1	1.37 + 0
1.70 + 1	5.41 - 1
1.26 + 1	1.86 - 1
5.01 + 0	3.75 - 2
2.44 + 0	2.01 - 2
2.65 - 1	1.69 - 2
3.54 - 2	4.28 - 3

The smallest eigenvalue for the normalized case was then eliminated by removing the diffraction data for one of the aperture sizes. The selection of the data to be removed was again based on an examination of the covariance matrix G^TG. This indicated that the data for the 80 μm aperture were more nearly linear combinations of the data for the other aperture sizes than any of the other data. Therefore, the diffraction data for the 80 μm aperture were removed and the eigenvalues of the normalized data were calculated again.

The results are indicated in Table 16 along with the preceding results. These eigenvalues indicate that the selection of basis sizes is good inasmuch as the range of the eigenvalues is minimized and the size interval from 10 to 90 μm diameter is resolved into the largest number of size intervals compatible with minimizing the range of eigenvalues.

TABLE 16

RESULTS OF ELIMINATION OF DIFFRACTION PATTERN DATA FOR ONE PINHOLE

Ordered Eigenvalues of Normalized Data			
Including 80 μm Data		Excluding 80 μm Data	
Aperture Diameter (μm)	Ordered Eigenvalues	Aperture Diameter (μm)	Ordered Eigenvalues
10	5.83 + 0	10	4.98 + 0
25	1.37 + 0	25	1.21 + 0
35	5.41 - 1	35	5.25 - 1
50	1.86 - 1	50	1.77 - 1
60	3.75 - 2	60	3.64 - 2
70	2.01 - 2	70	2.00 - 2
80	1.69 - 2	90	1.51 - 2
90	4.28 - 3		

In Table 17 the above results are compared with the computer-simulation results described above for the selection of particle size intervals based on the criterion that the diffraction patterns of adjacent particle sizes intersect at 95% of their peak value. This table represents a direct comparison of the results obtained under ideal conditions by computer simulation with the results obtained by experimental measurements. Both results are compatible and indicate that the diffraction pattern technique will work theoretically and experimentally for sizing apertures. These results also indicate that the optimum condition under which the technique will work is that the size distribution of the sample to be measured should be similar to the graph of the normalization constants vs. aperture diameter. This will assure optimum size- and number-resolution.

The photographic samples consisted of transparencies with black circular spots located randomly on the transparencies. The spots were made by photographing monochromatic light passing through small holes drilled

TABLE 17

COMPARISON OF EXPERIMENTAL AND COMPUTER-SIMULATION RESULTS

Computer Simulation			Measured Pinhole Data		
Particle Diameters (μm)	Normalization Constants	Ordered Eigenvalues	Aperture Diameter (μm)	Normalization Constants	Ordered Eigenvalues
9.5	3.25 - 1	4.00 + 0	10	3.77 + 0	3.98 + 0
20.0	4.61 - 2	1.24 + 0	25	3.52 - 1	1.21 + 0
28.0	2.19 - 2	4.90 - 1	35	2.32 - 1	5.25 - 1
38.0	1.11 - 2	1.87 - 1	50	1.08 - 1	1.77 - 1
54.0	5.07 - 3	6.73 - 2	60	5.35 - 2	3.64 - 2
84.4	1.87 - 3	1.67 - 2	70	3.83 - 2	2.00 - 2
			90	3.56 - 2	1.51 - 2

through a thin sheet of metal. The monochromatic light was obtained by using a green filter between an intense light source and the sheet metal original. The distance between the source and the sheet metal was large enough to insure uniform illumination of all the circular holes. The distance from the original to the camera was adjusted to provide the desired spot size on the transparency. Thus, only one original was needed to produce a number of monodisperse samples of any size in the range from 17 to 100 μm. A significant reduction in spot size would have required more effort than could be justified for this initial investigation. Each time more holes were drilled through the sheet metal plate, a set of transparencies was made with the camera at various distances to cover the size range of interest. After development the spots were checked under a microscope for size and quality before more holes were drilled in the original.

A few polydisperse samples were produced by drilling larger holes through the original after the desired monodisperse samples had been obtained. Also, both mono- and polydisperse samples of transparent apertures in a black background were produced by a similar technique. Stick-on opaque circular paper discs of different sizes were obtained and placed on sheets of clear Mylar to serve as originals. The negative transparencies obtained from these originals then consisted of arrays of transparent circular spots on a black background.

Many attempts were made to measure the diffraction patterns produced by the transparency samples consisting of black spots on a clear background. However, the influence of the undiffracted incident light predominated

to such an extent that no data were obtained for calculating an inversion matrix and the associated eigenvalues. The basic difficulty was that a large portion of the incident light was not diffracted by the simulated particles and so was focused at the center of the otherwise weak diffraction pattern. Reflections of even small percentages of this undiffracted light predominated over the useful signal at the detector. The largest reflection occurred at the detector itself, because not all of the incident energy is absorbed by the detector material. Also, this detector array was fabricated by a technique that required a window between the incident light and the detector elements. Reflections from this window produced a strong halo of light incident on the detector elements. The correction procedure suggested by the detector manufacturer was found to be of no help. Their more recent detector arrays are fabricated without windows, which eliminates the problem of halos.

Other techniques for eliminating the undesired light were tried. The most successful was the use of an optical fiber at the focal point of the undiffracted light. However, even this method was only partly successful. The fiber collected most of the undesired light and directed it away from the detector, but there was still too much undesired light incident on the detector array. A part of this was found to be generated by reflections from the supposedly antireflection-coated Fourier transform lens. Tropel claimed that over 99% of the light incident on the lens should be transmitted. Our measurements indicated that only about 84% of the incident light at the design wavelength of 0.488 μm was transmitted and at least a large part of the other 16% was reflected at lens-air interfaces inside the multi-element transform lens. The lens was returned to Tropel and found by them to be defective. At any rate, our initial attempts to measure the diffraction patterns of low number-density opaque particles on a transparent background have not yielded data suitable for calculating an inversion matrix. The simpler case of transparent circular apertures on an opaque background did yield data which were used to calculate an inversion matrix and the related eigenvalues. The resulting eigenvalues are indicated in Table 18. The first column indicates the diameter of the pinholes in the monodisperse samples. The second column indicates the number of pinholes of each size that produced the measured diffraction patterns. The third column consists of the ordered eigenvalues calculated from the data before the final normalization. These data were already partially normalized by the use of larger numbers of pinholes for smaller pinhole diameters. The most interesting feature in this Table is the comparison of the results before and after normalization. It is seen that before normalization the smallest eigenvalue was three decades smaller than the next larger eigenvalue. After normalization all six eigenvalues occurred within a range of about two decades. This indicated again that it should be possible to trade off particle-number resolution at the small end of the particle size range in order to improve the particle-size resolution.

TABLE 18

EXPERIMENTAL RESULTS FROM PHOTOGRAPHIC SAMPLES

Results Before Normalization			After Normalization	
Aperture Diameter (μm)	Number	Ordered Eigenvalues	Ordered Eigenvalues	Normalization Constants
14	114	3.56 + 2	4.17 + 0	3.26
20	50	5.98 + 1	1.28 + 0	0.362
28	24	6.83 + 0	3.86 - 1	0.121
38	12	4.51 + 0	1.00 - 1	0.120
54	6	2.93 + 0	5.20 - 2	0.148
84	2	2.86 - 3	1.37 - 2	0.065

Only one test of the inversion matrix technique for counting and sizing particles was completed with experimental data. The results to be described should be taken more as an example of the procedure used rather than as an example of the accuracy of the technique. With more experience in applying the technique, and improvements in the optical system, the accuracy should be improved.

The data from the monodisperse pinhole arrays described above were used to calculate an inversion matrix. However, the diffraction data for the smallest particles (14 μm diameter) were removed because of the unusually large value required for normalization (see Table 18). The inversion matrix was calculated and used as a multiplier to invert the diffraction pattern produced by a polydisperse pinhole array. The results of the matrix multiplication and the conversions required to account for the normalization are shown in Table 19. The lefthand column indicates the aperture diameter at the center of each size interval of the inversion matrix. The second column is the result of multiplying the measured diffraction pattern data by the previously calculated inversion matrix. The third and fourth columns indicate the number of pinholes in the monodisperse samples and the constants used to normalize the monodisperse data for calculating the inversion matrix. The fifth column, the number of pinholes calculated, is the product of the second, third, and fourth columns. As a comparison, the known data for the polydisperse sample are indicated in the two right-most columns.

The first thing to be noted is that the matrix inversion technique should work best for samples in which the particle number density is large and for which the size distribution is a continuous function that is parallel to

TABLE 19

APPLICATION OF EXPERIMENTALLY DERIVED INVERSION MATRIX TO MEASURED DIFFRACTION PATTERN DATA

Aperture Diameter (μm)	Inversion Matrix x Diffraction Pattern	Monodisperse Data Number of Pinholes	Monodisperse Data Normalization Constant	Number of Pinholes Calculated	Polydispersion No.of Pinholes	Polydispersion Diameter (μm)
20	0.819	50	0.362	14.8	10	14.6
28	1.61	24	0.121	4.68	-	-
38	3.02	12	0.120	4.35	5	36.6
54	4.67	6	0.148	4.15	2	57.1
84	2.19	2	0.065	0.28	1	76.4

a graph of the product of the normalization constants multiplied by the number of apertures in the monodisperse samples. These conditions were not met in this test, which may account for some of the discrepancy between the "number of pinholes calculated" and the "number of pinholes" known to be in the polydispersion.

Another point that should be noted is the fact that the "number of pinholes calculated" was always positive. For several analogous computer simulation tests this was not true, particularly when the eigenvalues related to the inversion matrix covered a wide range. As indicated earlier, the eigenvalues associated with this experimentally derived inversion matrix lay within a relatively small range. Remembering that this was the first experimental test of the matrix inversion technique, the results were quite satisfactory.

At the end of the experimental work on this Grant a unique detector array became available for a short time. This was the fiber-optic/photodiode array constructed by Georgia Tech for NASA [9] and described earlier. The minicomputer associated with this array was able to store the background signal levels and subtract these from signal-plus-background data to yield the corrected diffraction pattern in real-time. This greatly facilitated the examination of diffraction patterns from a variety of samples.

Even though an inversion matrix was not derived for this detector array the size of dense monodisperse samples was calculated from the measured position of the first null in the diffraction patterns. The samples studied consisted of those described earlier as well as an assortment of materials deposited on microscope slides. The spray from an aerosol can will also produce a measurable diffraction pattern. However, this pattern was characteristic of a polydispersion with a broad size distribution. This would have required an inversion matrix for analysis of the size distribution.

REFERENCES

1. Goodman, Joseph W., Introduction to Fourier Optics, McGraw-Hill, New York (1968).

2. Jenkins, Francis A. and Harvey E. White, Fundamentals of Optics, 3rd ed., McGraw-Hill, New York (1957).

3. Hecht, Eugene and Alfred Zajac, Optics, Addison-Wesley, Massachusetts (1974).

4. Van de Hulst, H. C., Light Scattering by Small Particles, Wiley, New York (1957).

5. Anderson, W. L. and R. E. Beissner, "Counting and Classifying Small Objects by Far-Field Light Scattering," Applied Optics, 10, 1503 (1971).

6. Noble, Ben, Applied Linear Algebra, Prentice-Hall, New Jersey (1969).

7. Twomey, S. and H. B. Howell, "Some Aspects of the Optical Estimation of Microstructure in Fog and Cloud," Applied Optics, 6, 2125 (1967).

8. Dave, J. V., "Determination of Size Distribution of Spherical Polydispersions Using Scattered Radiation Data," Applied Optics, 10, 2035 (1971).

9. McSweeney, A., "Design and Fabrication of an Engineering Model Fiber-Optics Detector," Final Report, Contract NAS8-28215, (1972).

BIBLIOGRAPHY

Aughey, W. Henry and F. J. Baum. Angular-dependence light scattering - a high-resolution recording instrument for the angular range 0.05 -140°. J. Opt. Soc. Am., 44, 833 (1954).

Backus, G., and F. Gilbert. Uniqueness in the inversion of inaccurate gross earth data. Philos. Trans. Roy. Soc. London, 266, 123 (1970).

Bailey, Adrian G. Review: The generation and measurement of aerosols. Journal of Materials Science, 9, 1344 (1974).

Chin, J. H., C. M. Sliepcevich, and M. Tribus. Particle size distributions from angular variation of intensity of forward-scattered light at very small angles. J. or Physical Chem., 59, 851 (1955).

Cornillault, J. Particle Size Analyzer. Applied Optics, 11, 265 (1972).

Curico, Joseph A. Evaluation of atmospheric aerosol particle size distribution from scattering measurements in the visible and infrared. J. Opt. Soc. Am., 51, 548 (1961).

Deirmendjian, D. Scattering and polarization properties of water clouds and hazes in the visible and infrared. Applied Optics, 3, 187 (1964).

Farmer, W. M. Measurement of particle size, number density, and velocity using a laser interferometer. Applied Optics, 11, 2603 (1972).

Farmer, W. M. Observation of large particles with a laser interferometer. Applied Optics, 13, 610 (1974).

Faxvog, Frederick R., Detection of airborne particles using optical extinction measurements. Applied Optics, 13, 1913 (1974).

Ferrara, R., G. Fiocco, and G. Tonna. Evolution of the fog droplet size distribution observed by laser scattering. Applied Optics, 9, 2517 (1970).

Fourney, M. E., J. H. Matkin, and A. P. Waggoner. Aerosol size and velocity determination via holography. The Review of Scientific Instruments, 40, 205 (1969).

Grassl, H. Determination of aerosol size distributions from spectral attenuation measurements. Applied Optics, 10, 2534 (1971).

Grum, F., D. J. Paine, and J. L. Simonds. Prediction of particle-size distributions from spectrogoniophotometric measurements. J. Opt. Soc. Am., 61, 70 (1971).

Gumprecht, R. O. and C. M. Sliepcevich. Scattering of light by large spherical particles. J. of Phys. Chem., 57, 90 (1953).

Hodkinson, J. Raymond. Particle sizing by means of the forward scattering lobe. Applied Optics, 5, 839 (1966).

Holland, A. C. and G. Gagne. The scattering of polarized light by polydisperse systems of irregular particles. Applied Optics, 9, 1113 (1970).

Jones, A. R. Light scattering by a sphere situated in an interference pattern, with relevance to fringe anemometry and particle sizing. J. Phys. D: Appl. Phys., 7, 1369 (1974).

Kaye, Wilbur and A. J. Havlik. Low angle laser light scattering - absolute calibration. Applied Optics, 12, 541 (1973).

Kerker, Milton. The scattering of light and other electromagnetic radiation. Academic Press, New York (1969).

Lanczos, Cornelius. Applied analysis. Prentice Hall, New Jersey (1956).

Livesey, P. J. and F. W. Billmeyer, Jr. Particle-size determination by low-angle light scattering: New instrumentation and a rapid method of interpreting data. Journal of Colloid and Interface Science, 30, 447 (1969).

Mateer, Carlton L. On the information content of umkehr observations. Journal of the Atmospheric Sciences, 22, 370 (1965).

Meehan, E. J. and A. E. Gyberg. Particle-size determination by low-angle light scattering: Effect of refractive index. Applied Optics, 12, 551 (1973).

Mullaney, P. F. and P. N. Dean. Cell sizing: A small-angle light-scattering method for sizing particles of low relative refractive index. Applied Optics, 8, 2361 (1969).

Myers, Mark E., Jr., and Andrew M. Wims. Elimination of speckle noise in laser light scattering photometry. Applied Optics, 11, 947 (1972).

Phillips, David L. A technique for the numerical solution of certain integral equations of the first kind. Journal of the Association for Computing Machinery, 9, 84 (1962).

Pinnick, R. G. and D. J. Hofmann. Efficiency of light-scattering aerosol particle counters. Applied Optics, 12, 2593 (1973).

Powell, R. S. R. R. Circle, D. C. Vogel, P. D. Woodson III, and Bertram Donn. Optical scattering from non-spherical randomly aligned, polydisperse particles. Planet. Space Sci., 15, 1641 (1967).

Proctor, T. D. The use of a gas laser for sizing single particles of airborne dust. J. Phys. Sect. E, 5, 1226 (1972).

Rinard, Phillip M. Determination of particle size by diffraction of light. Am. J. of Physics, 42, 320 (1974).

Roess, L. C. A simple method of obtaining a particle mass distribution by inverting the x-ray intensity scattered at small angle. J. of Chemical Physics, 14, 695 (1946).

Rust, B., W. R. Burrus, and C. Schneeberger. A simple algorithm for computing the generalized inverse of a matrix. Communication of the ACM, 9, 381 (1966).

Saylor, Charles Proffer. A study of errors in the measurement of microscopic spheres. Applied Optics, 4, 477 (1965).

Schehl, R., S. Ergun, and A. Headrick. Size spectrometry of aerosols using light scattering from the cavity of a gas laser. Rev. Sci. Instrum., 44, 1193 (1973).

Spankuch, Dietrich. Information content of extinction and scattered-light measurements for the determination of the size distribution of scattering particles. Applied Optics, 11, 2844 (1972).

Stark, H., W. R. Bennett, and M. Arm. Design considerations in power spectra measurements by diffraction of coherent light. Applied Optics, 8, 2165 (1969).

Steinkamp, J. A., M. J. Fulwyler, J. R. Coulter, R. D. Hiebert, J. L. Horney, and P. F. Mullaney. A new multiparameter separator for microscopic particles and biological cells. Rev. Sci. Instrum., 44, 1301 (1973).

Stigliani, Daniel J., Raj Mittra, and Richard G. Semonin. Particle-size measurement using forward-scatter holography. J. Opt. Soc. Am., 60, 1059 (1970).

Strand, Otto Neall and Ed R. Westwater. Statistical estimation of the numerical solution of a fredholm integral equation of the first kind. Journal of the Association for Computing Machinery, 15, 100 (1968).

Thompson, Brian J., John H. Ward, and William R. Zinky. Application of hologram techniques for particle size analysis. Applied Optics, 6, 519 (1967).

Thompson, Brian J. and William R. Zinky. Holographic detection of submicron particles. Applied Optics, 7, 2426 (1968).

Trolinger, J. D., R. A. Belz, and W. M. Farmer. Holographic techniques for the study of dynamic particle fields. Applied Optics, 8, 957 (1969).

Turner, F. M. and L. F. Radke. The design and evaluation of an airborne optical ice particle counter. J. of Applied Technology, 12, 1309 (1973).

Twomey, S. Information content in remote sensing. Applied Optics, 13, 942 (1974).

Twomey, S. On the numerical solution of fredholm integral equations of the first kind by the inversion of the linear system produced by quadrature. Journal of the Association for Computing Machinery, 10, 97 (1963).

Twomey, S. The application of numerical filtering to the solution of integral equations encountered in indirect sensing measurements. Journal of the Franklin Institute, 279, 95 (1965).

Twomey, S. and H. B. Howell. A discussion of indirect sounding methods with special reference to the deduction of vertical ozone distribution from light scattering measurements. Monthly Weather Review, 659 (Oct.-Dec. 1963).

Twomey, S. and G. T. Severynse. Measurements of size distributions of natural aerosols. Journal of the Atmospheric Sciences, 20, 392 (1963).

Westlake, J. R. A handbook of numerical matrix inversion and solution of linear equations. Wiley, New York (1968).

Westwater, E. R. and A. Cohen. Application of Backus-Gilbert inversion technique to determination of aerosol size distributions from optical scattering measurements. Applied Optics, 12, 1340 (1973).

Wims, Andrew and Mark E. Myers, Jr. An automated, laser light-scattering photometer (0.1 to 170° range) with a single photon counting system. Journal of Colloid and Interface Science, 39, 447 (1972).

Yamamoto, Giichi and Masayuki Tanaka. Determination of aerosol size distribution from spectral attenuation measurements. Applied Optics, 8, 447 (1969).

TECHNICAL REPORT DATA
(Please read Instructions on the reverse before completing)

1. REPORT NO.	2.	3. RECIPIENT'S ACCESSION NO.
4. TITLE AND SUBTITLE A DIFFRACTION TECHNIQUE TO MEASURE SIZE DISTRIBUTION OF LARGE AIRBORNE PARTICLES		5. REPORT DATE 6. PERFORMING ORGANIZATION CODE
7. AUTHOR(S) A. McSweeney		8. PERFORMING ORGANIZATION REPORT NO.
9. PERFORMING ORGANIZATION NAME AND ADDRESS Georgia Institute of Technology Engineering Experiment Station Atlanta, GA 30332		10. PROGRAM ELEMENT NO. 110302 11. CONTRACT/GRANT NO. R-802214
12. SPONSORING AGENCY NAME AND ADDRESS Environmental Sciences Research Laboratory Office of Research and Development U.S. Environmental Protection Agency Research Triangle Park, North Carolina 27711		13. TYPE OF REPORT AND PERIOD COVERED Final Report 12/73 - 12/75 14. SPONSORING AGENCY CODE EPA-ORD
15. SUPPLEMENTARY NOTES		

16. ABSTRACT

The purpose of this project is to test and demonstrate a coherent optical diffraction technique for measuring the size distribution of large particles. This technique is based on the generation of a transformation matrix which is used to relate the measured diffraction patterns to the size distribution of the samples that produced the patterns.

Four types of samples are considered: 1) pinholes in opaque discs, 2) photographic transparencies with opaque circular spots, 3) particles deposited on microscope slides, and 4) aerosols. Computer simulations are performed to assess the accuracy and resolution of the techniques.

Although good results are obtained for pinholes in opaque discs, experimental difficulties limit the precision of this techniques applied to particles in a transparent medium. Improvements based on a reduction of system noise and an increase in detector sensitivity are discussed and applied to the requirements on number density and size range of particles in a transparent medium.

17. KEY WORDS AND DOCUMENT ANALYSIS

a. DESCRIPTORS	b. IDENTIFIERS/OPEN ENDED TERMS	c. COSATI Field/Group
* Air pollution		13B
* Aerosols		07D
* Diffraction		20F
* Particle size distribution		20E
Lasers		

18. DISTRIBUTION STATEMENT RELEASE TO PUBLIC	19. SECURITY CLASS *(This Report)* UNCLASSIFIED 20. SECURITY CLASS *(This page)* UNCLASSIFIED	21. NO. OF PAGES 57 22. PRICE

EPA Form 2220-1 (9-73)